Towards High-Rate Fabrication of Photonic Devices Utilizing a Combination of Roll-To-Roll Compatible Imprint Lithography and Ink Jet Printing Methods

Xiaohui Lin[a], Tao Ling[b], Harish Subbaraman[c], L. Jay Guo[b] and Ray T. Chen[*,a]

[a] Department of Electrical and Computer Engineering, The University of Texas at Austin, Austin, TX, 78758, USA

[b] University of Michigan, Department of Electrical Engineering and Computer Science, Ann Arbor, MI 48109, USA

[c] Omega Optics, Inc., 10306 Sausalito Dr, Austin, TX 78759, USA

ABSTRACT

Traditionally, polymer photonic devices are fabricated using clean-room processes such as photolithography, electron beam lithography, reactive ion etching (RIE) and lift-off methods etc, which leads to long fabrication time, low throughput and high cost. We describe in this paper a novel process for fabricating polymer photonic devices using a combination of imprinting and ink jet printing methods, which provides high throughput on a variety of rigid and flexible substrates with low cost. Particularly, we demonstrate a thermo-optic switch and an electro-optic modulator. In the rib waveguide patterning, the imprint lithography transfers the waveguide pattern from a soft mold to UV-15LV bottom cladding layer. The soft mold is replicated from a silicon master mold and rendered hydrophobic to ensure successful de-molding. Ink jet printing method is used to deposit the core layer in thermo-optic switch and electrode layers in electro-optic modulator. Compared to spin-coating method, the use of print-on-demand method greatly reduces material consumption and process complexity. Every step involved has the potential to be fully compatible with roll-to-roll (R2R) volume production. For example, the soft mold can be wrapped around a cylinder to realized roll-to-roll imprinting. By combining R2R imprint lithography with ink jet printing, fabrication of large volume and large area multi-layer polymer photonic devices can be realized.

Keywords: imprint lithography, ink jet printing, thermo-optic switch, electro-optic modulator, roll-to-roll

1. INTRODUCTION

Polymer material provides an excellent platform for demonstrating various kinds of active and passive optical devices, including optical bus waveguides [1], optical switches [2, 3], optical modulators [4-6], etc. The traditional method for polymer optical device fabrication includes using photolithography or electron beam lithography to create the pattern into a resist, and further transferring the pattern to the optical polymer via reactive ion etching process. This method is straightforward, but not a cost-effective way due to complicated fabrication process and low throughput. Another method is to directly pattern a low loss UV-curable polymer using photo-lithography [7]. However, this method is limited due to poor dimension and profile control resulting from the effects of wave diffraction, interface and substrate scattering [8]. Alternatively, imprinting technique can effectively overcome these shortcomings and provide the potential for high-rate roll-to-roll patterning capabilities at both micro- and nano-scales. Several optical components and devices have been demonstrated using various imprinting techniques, including EO polymer modulator[9], micro-lens arrays[10], micro-ring resonators[11], LEDs[12], polarizers[13], etc. However, despite utilizing imprinting to define the pattern, other processes (such as spin coating, evaporation, etching and lift-off) are still used in the fabrication process, which will increases the process complexity and cost. Therefore, we worked towards achieving all-printable optical devices, especially optical switch and modulator. In the present work, in addition to a UV based imprinting method which defines

* Ray T. Chen: chen@ece.utexas.edu

Advanced Fabrication Technologies for Micro/Nano Optics and Photonics VI, edited by Georg von Freymann, Winston V. Schoenfeld, Raymond C. Rumpf, Proc. of SPIE Vol. 8613, 86131H · © 2013 SPIE
CCC code: 0277-786X/13/$18 · doi: 10.1117/12.2005132

the waveguide channel with great repeatability, an ink jet printing method is also integrated in the process to deposit certain layers. A combination of imprinting and ink jet printing techniques can lead to advanced roll-to-roll fabrication process that enables high speed, low cost device fabrication. Especially, from material consumption point of view, inkjet printing only deposits material at the desired region, thus minimizing both material consumption and wastage, compared with spin coating method. Also, it is featured by aligned printing, which reduces the complicated steps of lithography and lift-off.

In this paper, utilizing the precise structural patterning capabilities of imprinting method, and integrating precise material placement advantages offered by ink-jet printing technique in the process flow, we successfully demonstrated a 2×2 thermo-optic (TO) switch and a Mach-Zehnder based electro-optic (EO) modulator. For the TO switch, its operation up to 1 kHz is demonstrated experimentally. For the EO modulator, up to 100 kHz modulation signal is presented. To our knowledge, this is the first demonstration of the key components in polymer photonics using printing processes. Furthermore, this roll-to-roll (R2R) compatible printing processes will be able to provide a great potential solution for the development of flexible and low cost integrated photonic devices with high yield.

2. MATERIAL SYSTEM SELECTION

In order to enable device development, the material system choice should meet certain criteria: First, all the materials should satisfy the optical index requirement to form a waveguide. Second, the bottom cladding layer should be imprintable. Third, the material should have suitable viscosity and surface tension to be ink jetted. The printer employed in this research is a Fujifilm Dimatix Materials Printer (DMP-2800). It utilizes a piezoelectric cartridge to jet material onto a desired area on the substrate. The printable material should have its viscosity between 10-12 cPs ($1.0x10^{-2}$ - $1.2x10^{-2}$ Pa·s) and surface tension between 28 and 33 dynes/cm (0.028 - 0.033 N/m) at operating temperature. For TO device, there is extra requirement that the core layer should have sufficient thermo-optic coefficient so that a suitable change in the index is achieved within a small temperature gradient. For EO device, the layers surrounding EO polymer should be compatible with it otherwise it will degrade the performance of EO polymer. Based on the above constraints, we determine the material selections as follows.

For TO switch, we selected UV15LV (n=1.501@1.55μm) from MasterBond as the bottom cladding layer, SU8-2000.5 (n=1.575@1.55μm) from MicroChem as the core layer and UFC-170A (n=1.496@1.55μm) from URAY Co. Ltd as top cladding layer. Of the three layers, the bottom cladding material UV15LV and the core layer material SU-8 2000.5 are ink-jet printable. Although LFR/ZPU series TO polymer from ChemOptics, Korea, with its high TO coefficient of ~ -2.5 x 10^{-4}/K @1.55μm, is an ideal choice for TO polymer switch development [3, 14, 15], its relatively lower refractive index (n < 1.48) compared to UV15LV, rules out its use as a core material. Moreover, the wide availability, low cost, great stability and higher refractive index of SU-8 polymer are beneficial for low cost polymer device development in spite of its lower TO coefficient of -1.1 x 10^{-4}/K @1.55μm.

For EO modulator, we selected UV15LV as the bottom cladding layer, EO polymer (AJ-CKL1, n=1.63@1.55μm) as the core layer and UFC-170A (n=1.496@1.55μm) from URAY Co. Ltd as top cladding layer. The choice of cladding materials is mainly based on the rigorous requirement of EO polymer because it is not compatible with solvent-based materials. UV15LV is a solvent-free polymer, and gets cross linked when exposed to UV. Besides, UV15LV is also an ink-jet printable material, thus having the potential to be deposited by ink-jet printing method in the roll-to-roll system. For the electrode layers, commercially available silver nanoparticle ink from Cabot Corp. was chosen.

3. THERMO-OPTIC SWITCH

1.1 Design and simulation

A schematic of the 2×2 thermo-optic polymer TIR switch is shown in Figure 1(a). The design of the switch includes two major parts: the optical design and the thermal design. The optical path and waveguide cross section are designed and simulated, as shown in Figures 1(a)-(c), with a horn structure. A rib waveguide structure is used and the core layer consists of a 1.8 μm thick slab and a 5 μm (width) × 0.5 μm (thick) strip. The separation of two input and two output waveguides is set at 250 μm, which is compatible with a standard fiber array. A curved waveguide with 10mm bending radius is used to guide light from the input port to the X junction. A horn structure [16] is used at the junction, with a maximum width of 40 μm at the center. The half branch angle for the X junction is optimized at 4^{o} based on the consideration of cross-talk minimization and switching power trade-off. Larger junction angle requires more power to switch the light while smaller junction angle will increase the cross-talk between two ports. Besides, the horn structure is

also compatible with the temperature gradient generated by the heating element. The heating element is designed to have a width of 8 μm at the center. Due to its thinness compared to other connecting parts, most of heat is generated at the center region only. Due to the relatively thin electrode, when heated up, the temperature difference between the electrode and the SU-8 layer is less than 5°C, according to simulation. If it is assumed that only the polymer layers beneath the heating electrode undergo a change in refractive index, a -0.02 index change in the SU-8 layer is needed for reflecting all of the input light from one arm to the other at the X junction. Since SU-8 has a thermo-optic coefficient of -1.1×10^{-4}/K, the temperature change required is over 180°C. However, in reality, the heat distribution beneath the electrode takes a Gaussian profile. Therefore, the adjacent polymer will also get heated up, thus lower the temperature change required, and thus, the electrical power needed to total internally reflect the light. The simulated fundamental mode in the waveguide is shown in Figure 1(b), where the mode is well confined within the waveguide region and does not extend more than 3μm into the cladding, which helps in reducing the absorption loss from the gold heating electrode. The simulated powers in the bar (blue) and the cross (green) ports for the switching condition are also shown in Figure 1(c).

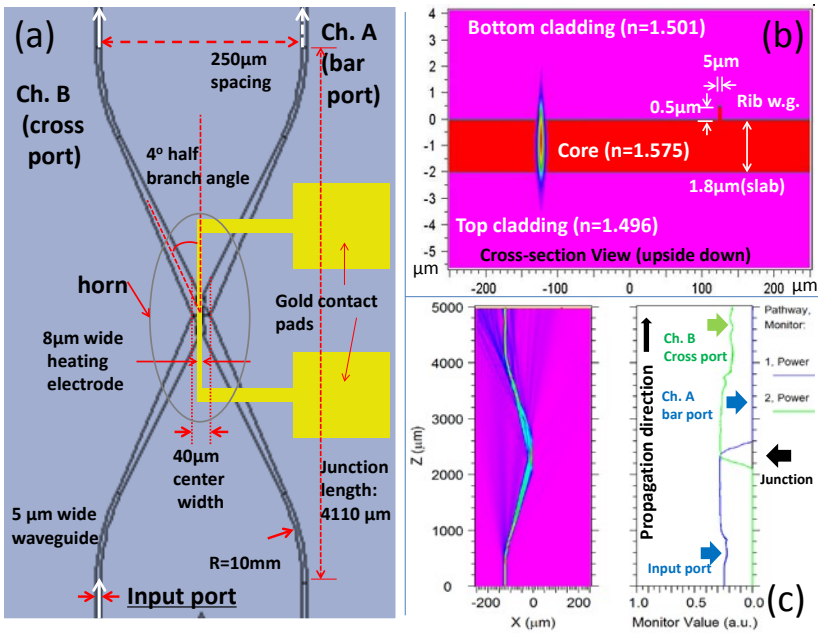

Figure 1(a) schematic showing the top view of the 2×2 thermo-optic switch layout. A horn structure, with a half branch angle of 4° is used. Gold heating electrode is 8 μm wide over the center region of the horn. (b) The cross-section view and the simulated mode profile at the input side of the 2×2 TO switch. The mode is well confined in the waveguide. Core layer is composed of 1.8 μm thick slab and 0.5 μm (height) x 5 μm (width) strip. (c) Simulation results of the power outputs from the bar (blue) and the cross (green) ports when the junction is in switching condition

1.2 Fabrication process

Traditionally, thermo-optic polymer TIR switches utilizing channel waveguide or rib waveguide structures are fabricated by photolithography and reactive ion etching process. The high energy bombardment in the reactive ion etching process is capable of removing polymer materials using photo-resist or metal as an etching mask. The disadvantages of this method include long fabrication time, low throughput and high cost. In the current work, the waveguide channel is generated by a flexible mold based UV nanoimprinting process, which could be compatible with roll-to-roll processing, and has the potential for high speed, low cost device fabrication. For the presented thermo-optic switch, besides imprinting, we also integrate an ink-jet printing method to deposit the core layer. The fabrication process flow is shown in Figure 2. First, a flexible mold is fabricated using a silicon hard mold. The flexible mold is then used to define the core region in a UV15LV bottom cladding layer, which is coated on a silicon substrate [Figure 2(b)]. Following this step, an ink-jet printer is used to print a layer of SU8, which not only fills the core trench, but also forms a planar top surface for further processing [Figure 2(c)]. Upon curing, another layer of UV15LV is ink-jet printed on top to form the top cladding layer. Please note that we have found the gold heater electrode fabrication process (lift-off method) incompatible with the printed UV15LV layer. Therefore, for demonstration purpose, we have chosen UFC-170A as a top cladding layer. In future, by switching to another R2R process for electrode transfer [17], UV15LV can replace UFC-

170A. Figure 2(f) and (g) show the top view microscopic picture and cross-section SEM image of the device, respectively.

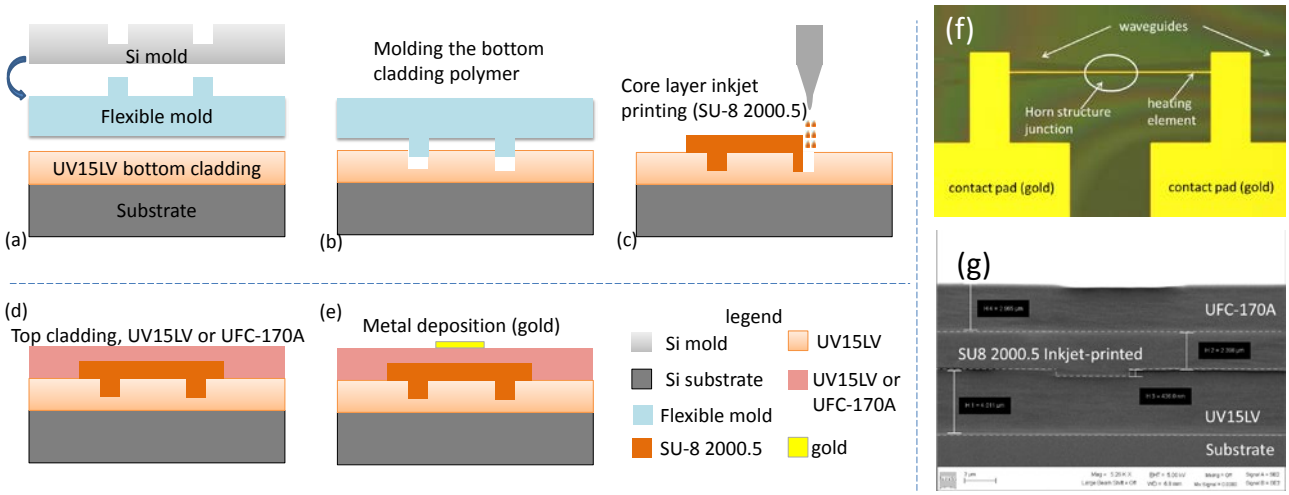

Figure 2 Process flow for fabricating a 2×2 thermo-optic polymer switch using imprinting and ink-jet printing method

1.3 Device testing

The testing is performed with the aid of auto aligner system. The input light at a wavelength of 1550nm wavelength is launched into one port of the device using a lensed fiber. A DC voltage from a power supply is applied across the heating elements using probes. An ammeter is used to monitor the real-time current, which is required in order to calculate the overall power consumption. To examine the performance of switching behavior at different applied voltages, output light power from two output channels of the device, as well as the current reading on the ammeter are recorded. It is measured that around 100mW power is needed for the cross port to reach its maximum output, which we define as switching power.

Response speed is another important parameter for a switch. A function generator is used to generate a square wave signal at different frequencies and applied across the heating electrode. The optical response at each frequency is measured using an oscilloscope, as shown in Figure 3. It can clearly be seen from the figure that device operates up to a frequency of 1 kHz. We also measured the rising/falling time of the device to be 0.46ms/0.40ms. The rising time for bar port and falling time for cross port are relatively longer because they correspond to the OFF state of the applied signal, wherein the junction needs more time to dissipate the heat, compared to the time needed to heat up the polymer.

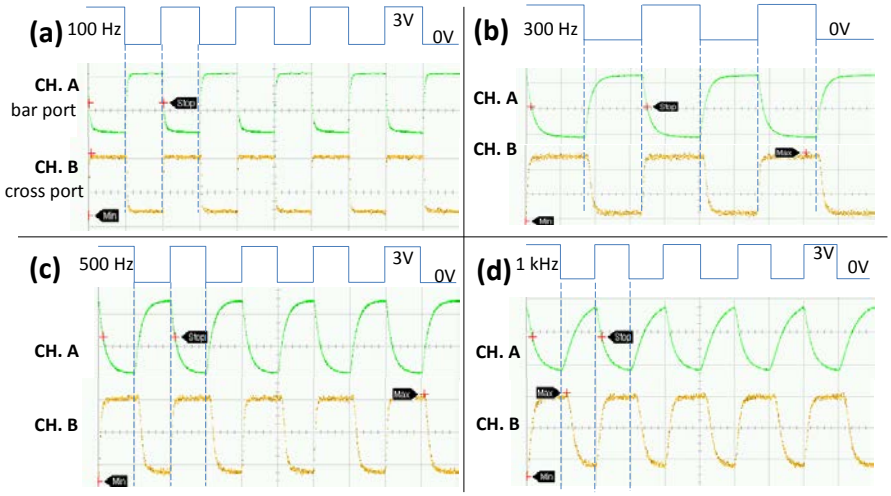

Figure 3 Optical response with square wave function applied across the heating electrode, at selected frequencies of (a) 100Hz, (b) 300Hz, (c) 500Hz, and (d) 1kHz. The device can operate at 1kHz with decent performance. Channel A represents bar port and Channel B represents cross port.

4. ELECTRO-OPTIC MODULATOR

1.4 Modulator design

A schematic of the Mach-Zehnder modulator we designed is shown in Figure 4. In our structure, we use an inverted rib waveguide structure to form the core. In the MZ modulator configuration, when a voltage is applied on one of modulating arms, the refractive index change in the EO polymer in that arm is governed by the equation $\Delta n=(-1/2)\cdot\gamma_{33}\cdot n^3\cdot(V/d)$ and the phase difference between two arms is given by $\phi=(2\pi/\lambda)\cdot\Delta n\cdot L$, where γ_{33} is the EO coefficient of the EO polymer, n is the refractive index of the EO polymer, V is the voltage applied, d is the separation between ground and top electrodes, and L is the modulation length. For our structure, the EO polymer (AJ-CKL1) has $\gamma_{33}=80pm/V$ and $n=1.63$. The electrode separation and arm length are designed to be $d=8.3\mu m$and $L=7.1mm$, respectively. The theoretical value of the half-wave switching voltage is calculated to be $V_\pi=(\lambda\cdot d)/(L\cdot\gamma_{33}\cdot n^3)=5.23V$.

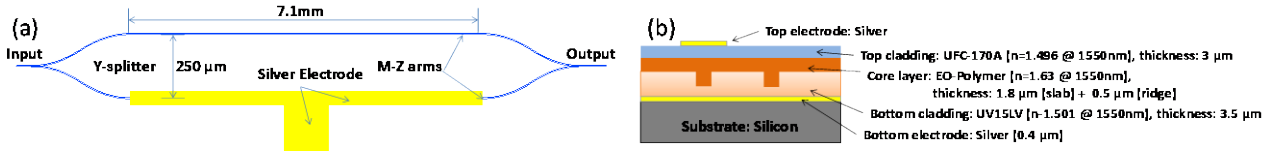

Figure 4 (a) Schematic top view showing the modulator structure, (b) Schematic cross section showing the different materials comprising the EO polymer modulator

1.5 Fabrication Process

The overall fabrication process flow is shown in Figures 5(a)-(e). First, a 350~400nm bottom silver electrode layer along with alignment marks on the substrate is ink-jet printed, as shown in Figure 5(a). Then, UV15LV is deposited onto the substrate to form bottom cladding layer, as shown in Figure 5(b). Next, a soft SSQ mold containing the MZ structure is brought into conformal contact with the bottom cladding layer. Then, a UV nanoimprinting process is performed to generate the waveguide trench into the UV15LV layer, followed by a demolding process, as shown in Figure 5(c). Upon completely curing the UV15LV layer, the EO polymer is coated, followed by top cladding UFC-170A deposition, to form a rib waveguide structure, as shown in Figure 5(d). Finally, a top silver electrode is ink-jet printed on top of the top cladding layer, and aligned to one arm of the MZ modulator waveguide with the aid of camera system and alignment mark located on both the ground electrode and the imprinted bottom cladding layers. With the aid of camera system, the misalignment can be controlled within 10µm. The inkjet-printed electrode serves as both a poling electrode and a driving electrode. Figures 5(f) and (g) show the optical microscope picture of a fabricated device and a zoom-in picture of the printed top electrode, respectively. The length of the top electrode is 7.1mm. Figure 5(h) shows an SEM cross-section image of all the layers that form the MZ modulator. As can be seen, the imprinted trench is filled with EO polymer, and the top and ground electrodes are uniformly deposited with the top electrode located right on top of the rib waveguide.

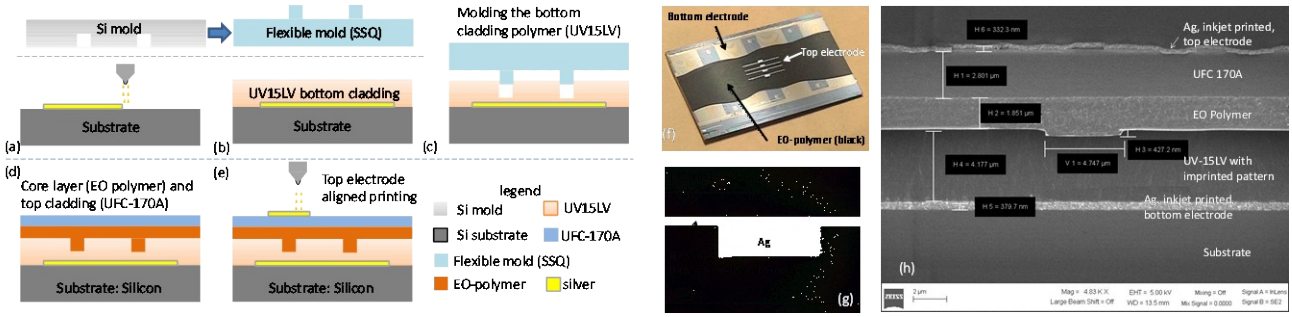

Figure 5 (a)-(e) Main process flow for fabricating an electro-optic polymer modulator using imprinting and ink-jet printing method. (f) printed EO polymer modulator, finished device (g) ink-jet printed top electrode (h) SEM picture showing the cross section of the modulator.

The electro-optic effect of EO polymer is created by contact poling process. Poling electric field of about 80V/µm is applied across the top and bottom silver electrodes. During the poling process, the temperature is controlled to increase from room temperature to peak poling temperature of 140°C, which is 5°C above the T_g of AJ-CKL1, and then quickly decreased back to room temperature. Throughout the entire poling process, leakage current is monitored by a

picoammeter. A current-limiting resistor and two back-to-back diodes are used in the circuit connection to protect the picoammeter from being damaged due to any unexpected high current induced breakdown.

1.6 Device testing

As shown in Figure 7(a), 1550nm TM-polarized laser is launched into the facet of the EO modulator. Driving signal is applied across the driving and ground electrodes of the device, and the modulated optical signal is then collected by a photodetector which is connected to an oscilloscope. The measured total insertion loss is around 26dB due to the high propagation loss of EO-polymer and the roughness of cleaved input and output facets. EO polymer has faster response to electrical field changing. Figure 7(b) and (c) show the input and modulator response when a 100 kHz saw-tooth wave is applied. The half wave switching voltage V_π is measured to be around 8.0V under 3kHz saw-tooth driving signal. It is higher than the calculated value probably due to the low poling efficiency of the EO polymer, which reduces the in-device γ_{33} value to *52.3 pm/V.* Higher voltages may increase the risk of device break down.

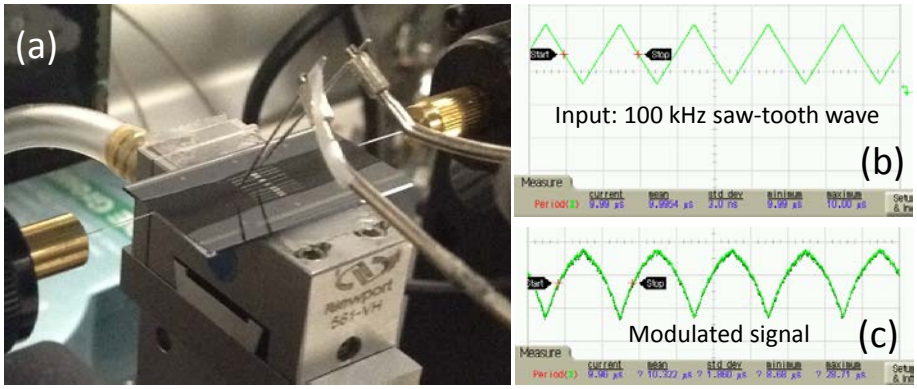

Figure 6 100 kHz saw-tooth signal input and corresponding modulator output signal. (c-d) 10 MHz sin wave input and corresponding modulator output.

5. CONCLUSION AND FUTURE WORK

The presented work explicitly demonstrates a novel fabrication technology for polymer based TO switch and EO modulator, taking advantage of UV imprinting to define waveguide patterns and ink-jet printing to deposit electro layers and waveguide layers. It greatly reduces the fabrication complexity and lowers the cost. Since both the imprinting and ink-jet printing method are roll-to-roll compatible, our technology provides a practical way for fabricating low cost flexible optical devices with high throughput. Future work will include the characterization of imprinting reliability in roll-to-roll situation and system development for multi-layer alignment strategy.

ACKNOWLEDGEMENTS

This work is supported by AFOSR STTR award FA9550-12-C-0052 supported by Dr. Gernot Pomrenke.

References

[1] X. H. Lin, X. Y. Dou, A. X. Wang *et al.*, "Polymer optical waveguide based bi-directional optical bus architecture for high speed optical backplane," Optoelectronic Interconnects Xii, 8267, (2012).

[2] H. Yu, X. Q. Jiang, J. Y. Yang *et al.*, "The design of 2x2 polymer TIR switch based on thermal field analysis employing thermo-optic effect," Passive Components and Fiber-Based Devices, Pts 1 and 2, 5623, 174-183 (2005).

[3] X. L. Wang, B. Howley, M. Y. Chen *et al.*, "4 x 4 nonblocking polymeric thermo-optic switch matrix using the total internal reflection effect," Ieee Journal of Selected Topics in Quantum Electronics, 12(5), 997-1000 (2006).

[4] B. S. Lee, C. Y. Lin, A. X. Wang *et al.*, "Demonstration of a Linearized Traveling Wave Y-Fed Directional Coupler Modulator Based on Electro-Optic Polymer," Journal of Lightwave Technology, 29(13), 1931-1936 (2011).

[5] D. H. Park, Y. Z. Leng, J. D. Luo *et al.*, "High speed electro-optic polymer phase modulator using an in-plane slotline RF waveguide," Rf and Millimeter-Wave Photonics, 7936, (2011).

[6] W. H. Steier, A. Szep, Y. H. Kuo *et al.*, "High speed polymer electro-optic modulators," Leos 2001: 14th Annual Meeting of the Ieee Lasers & Electro-Optics Society, Vols 1 and 2, Proceedings, 188-189 (2001).
[7] J. Y. Yang, Q. J. Zhou, and R. T. Chen, "Polyimide-waveguide-based thermal optical switch using total-internal-reflection effect," Applied Physics Letters, 81(16), 2947-2949 (2002).
[8] L. J. Guo, "Nanoimprint lithography: Methods and material requirements," Advanced Materials, 19(4), 495-513 (2007).
[9] G. T. Paloczi, Y. Huang, A. Yariv *et al.*, "Replica-molded electro-optic polymer Mach–Zehnder modulator," Applied Physics Letters, 85(10), 1662-1664 (2004).
[10] K. L. Lai, S. F. Hsiao, M. H. Hon *et al.*, "Patterning of polystyrene thin films by solvent-assisted imprint lithography and controlled dewetting," Microelectronic Engineering, 94, 33-37 (2012).
[11] T. Ling, S. L. Chen, and L. J. Guo, "Fabrication and characterization of high Q polymer micro-ring resonator and its application as a sensitive ultrasonic detector," Optics Express, 19(2), 861-869 (2011).
[12] P. C. Kao, S. Y. Chu, T. Y. Chen *et al.*, "Fabrication of large-scaled organic light emitting devices on the flexible substrates using low-pressure imprinting lithography," Ieee Transactions on Electron Devices, 52(8), 1722-1726 (2005).
[13] Y. Ekinci, H. H. Solak, C. David *et al.*, "Bilayer Al wire-grids as broadband and high-performance polarizers," Optics Express, 14(6), 2323-2334 (2006).
[14] Y.-T. Han, J.-U. Shin, S.-H. Park *et al.*, "N × N polymer matrix switches using thermo-optic total-internal-reflection switch," Opt. Express, 20(12), 13284-13295 (2012).
[15] Y. O. Noh, H. J. Lee, Y. H. Won *et al.*, "Polymer waveguide thermo-optic switches with - 70 dB optical crosstalk," Optics Communications, 258(1), 18-22 (2006).
[16] X. L. Wang, B. Howley, M. Y. Chen *et al.*, "Polymer based thermo-optic switch for optical true time delay," Integrated Optics: Devices, Materials, and Technologies IX, 5728, 60-67 (2005).
[17] M. G. Kang, and L. J. Guo, "Metal transfer assisted nanolithography on rigid and flexible substrates," Journal of Vacuum Science & Technology B, 26(6), 2421-2425 (2008).